Nonlocal theory for submerged cantilever beams undergoing torsional vibrations*

Burak Gulsacan , Matteo Aureli†
Mechanical Engineering Department
University of Nevada, Reno
1664 N Virginia St, Reno, NV 89557-0312

We propose a new theory for fluid-structure interactions of cantilever microbeams undergoing small amplitude vibrations in viscous fluids. The method is based on the concept of nonlocal modal hydrodynamic functions that accurately capture 3D fluid loading on the structure. For short beams for which 3D effects become prominent, existing local theories based on 2D fluid approximations are inadequate to predict the dynamic response. We discuss and compare model predictions in terms of frequency response functions, modal shapes, quality factors, and added mass ratios with the predictions of the local theory, and validate our new model with experimental results.

1 INTRODUCTION

Over the last few decades, vibrations of cantilever structures in viscous fluids have received intense research interest from the fluid-structure interaction (FSI) community, with applications in atomic force microscopy, sensing and actuation in micromechanical systems (MEMS), biomimetic robotic propulsion, piezoelectric fanning, and microscale energy harvesting systems [1–4]. Central to these studies, is the challenging estimation of the hydrodynamic forces on the vibrating solid structures. Arguably, the most fruitful approach has been that of [5, 6] which is based on the assumption of two dimensional (2D) unsteady Stokes flow around infinitely long beams, where only local transverse displacements are considered for a rigid cross section. The resulting local theory condenses the description of the hydrodynamic forces in a complex hydrodynamic function that can be used in structural dynamics models. This highly successful local theory has been shown to be accurate for the prediction of the first few flexural resonance frequencies and quality factors of slender submerged cantilevers.

Despite this success, recent interest has focused on applications of microplates and cantilevers with low aspect ratios [7] for which the local theory is inadequate. Recent studies [8, 9] have observed that traditional theories based on 2D fluid approximations or strip theory integration fail to capture the nonlocality of the fluid loading on the structure, which is important for low aspect ratios and high mode numbers.

The progress in the context of flexural vibrations in liquids has not been reflected on studies of torsional oscillations of beam-like structures in viscous fluids, which to date remain sparse. The seminal contribution in [10] provides the linear and local theory for torsional oscillation of submerged cantilever beams, relating the distributed hydrodynamic moment exclusively to the local twist of the beam axis and the nondimensional frequency of vibration, via a so-called complex hydrodynamic function. In [11], the local approach was expanded to finite amplitude vibrations, by incorporating a nonlinear correction to the hydrodynamic function. This correction captures the effect of vortex shedding and convective nonlinearities by augmenting the hydrodynamic moment with nonlinear hydrodynamic damping. While not specifically focused on torsion, in [12], a semi-numerical method was presented to investigate the FSI problem for a vibrating microcantilever plate underwater. Torsional modes were identified therein along with discrepancies from the local theory for lower aspect ratios. However, a truly nonlocal theory for torsional vibrations in viscous fluids has not been presented to date. As such, our understanding of this fundamental dynamics problem remains incomplete.

In this paper, we develop a three dimensional (3D) nonlocal theory for torsional vibrations of a submerged thin cantilever, by focusing on low aspect ratios structures undergoing small amplitude vibrations. Our method constitutes an "exact" solution, since the FSI problem is constructed in full 3D with only the assumption of thin cantilever. Therefore, effect of boundary conditions, finite aspect ratio, and nonlocality are naturally captured by this method. Our approach employs a semi-analytical FSI solver developed by our group based on the oscillatory Stokeslet theory [13, 14]. The FSI solution determines the distributed hydrodynamic loading resulting from the entire vibration profile of the cantilever. Such solution is then coupled to the traditional structural dynamics formalism via representation of the hydrodynamic operator on the basis of the structural modes. This leads to the new concept of the nonlocal modal hydrodynamic func-

*Paper presented at the 2023 Modeling, Estimation, and Control Conference (MECC 2023), Lake Tahoe, NV, Oct. 2-5. Paper No. MECC2023-76
†Address all correspondence to this author; maureli@unr.edu.

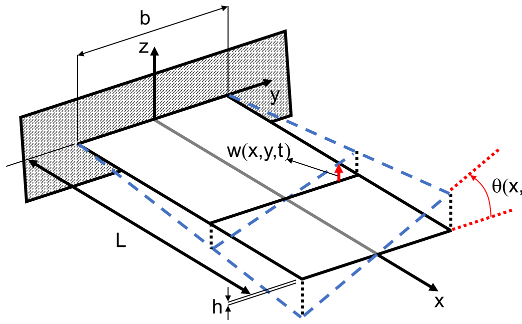

Fig. 1. Schematics and nomenclature of the problem. At any point, the transverse deflection is $w(x,y,t) = y\theta(x,t)$, with $\theta(x,t)$ the twist angle of the beam axis.

tion matrix. Importantly, the FSI problem is solved "offline" for a desired combination of geometry and dynamic parameters. As a result, our coupled method is computationally inexpensive, while retaining its "exact" semi-analytical nature. In fact, the only approximations in our method consist in the numerical discretization and can be controlled as desired.

For our novel theory, we present frequency response functions, modal shapes, quality factors, and added mass ratios and compare them with the predictions of the local theory. We also elucidate the nature of the nonlocal hydrodynamic function and the coupling of otherwise orthogonal structural modes via the fluid. This clarifies the importance of the off-diagonal terms of the modal hydrodynamic function matrix that have not been discussed before in the literature. Importantly, we verify our nonlocal theory with experimental results in the literature, demonstrating excellent agreement and predictive capabilities.

2 MODEL DEVELOPMENT

We consider a thin beam, submerged in a fluid, subjected to small-amplitude torsional vibrations. The beam is located in the xy-plane, while its length, width, and thickness are aligned with the x, y, and z axes, respectively. The time variable is indicated with t. The origin of the reference frame is at the centroid of the fixed cross-section at $x = 0$. We indicate length, width, and thickness of the plate as L, b, and h, respectively. We assume that $h \ll b$ so that the solid is modeled as a mathematical surface with zero thickness. The nomenclature and geometry of the problem are displayed in Fig. 1.

2.1 Governing equations

We use here the classical treatment of torsion for rectangular thin cross section beams, see for example [10, 11]. In this framework, torsion and other deformation modes, such as bending or extension, are decoupled. The beam density (mass per unit volume) is indicated with ρ_s. The beam is comprised of an isotropic and homogeneous material, with Young's modulus E and Poisson's ratio ν. The beam is subject to torsional vibrations along its axis x. The basic hypothesis is that the displacement field can be recovered from the axis twist angle $\theta(x,t)$ via the relation $w(x,y,t) = y\theta(x,t)$, see Fig. 1. Relevant static and stiffness property for the cross section are the moment of inertia $I_t = b^3h/12$ and the torsional stiffness GJ_t where $G = E/(2(1+\nu))$ is the shear modulus and $J_t = bh^3/3$ a geometric section property.

For underwater vibrations, we enrich the conventional equations of motion for the twist angle $\theta(x,t)$ of thin rectangular cross sections, with the nonlocal contribution of the surrounding fluid, that is,

$$GJ_t \frac{\partial^2\theta(x,t)}{\partial x^2} - \rho_s I_t \frac{\partial^2\theta(x,t)}{\partial t^2} = m_t(x,t) + \mathcal{H}^t[\theta(x,t)] \quad (1)$$

where $m_t(x,t)$ represents a moment (torque) per unit length along the axis of the beam. Eq. (1) is supplemented by fix-free boundary conditions. Here, $\mathcal{H}^t$ describes the hydrodynamic moment per unit length produced by the fluid-structure interactions as the beam axis is twisting with a time law $\theta(x,t)$. This is a linear but nonlocal term, and constitutes the novel contribution of this paper. This is also a substantial departure from the local approaches explored in [10, 11].

Focusing on steady state harmonic vibrations, we recast the problem in the frequency domain. Specifically, for a linear harmonic vibration problem occurring at the radian frequency ω, it is convenient to replace the physical twist angle with its phasor $\hat{\theta}(x,\omega)$, such that $\theta(x,t) = \mathrm{Im}\left[\hat{\theta}(x,\omega)e^{i\omega t}\right]$ with $i = \sqrt{-1}$, see for example [11]. Here and in the following, a superimposed hat indicates phasor quantities. In addition, we attack the equations of motion in the frequency domain via the Galerkin method, see [15], to rephrase the continuum problem in a finite-dimensional matrix formulation. Specifically, we rewrite the phasor of the twist angle as a superposition of "modes" as $\hat{\theta}(x,\omega) = \sum_i \hat{q}_i(\omega)\phi_i(x)$, where the $\hat{q}_i$ are modal coefficients to be determined and, as assumed modes, we select the in-vacuo modes of a fixed-free rod under torsion, that is, $\phi_i(x) = \sin(\lambda_i x/L)$ where $\lambda_i = (2i-1)\pi/2$ is an eigenvalue solution of the characteristic equation $\cos(\lambda_i) = 0$, see [15]. Note that these modes are arbitrarily scaled to unitary tip rotation.

Because of the linearity of the operators in Eq. (1), using the modal representation of the twist angle and projecting on the modes $\phi_j(x)$ yields a set of linear algebraic equations for the modal amplitudes in the form

$$\sum_i \int_0^L GJ_t\phi_i''\phi_j \mathrm{d}x\,\hat{q}_i - \omega^2\sum_i \int_0^L \rho_s I_t\phi_i\phi_j \mathrm{d}x\,\hat{q}_i = \int_0^L \hat{m}_t\phi_j \mathrm{d}x + \sum_i \int_0^L \mathcal{H}^t_\omega[\phi_i]\phi_j \mathrm{d}x\,\hat{q}_i \quad (2)$$

where a superimposed prime indicates derivative with respect to x and we have omitted the dependent variables for brevity. Importantly, $\mathcal{H}^t_\omega$ is the hydrodynamic moment nonlocal operator in the frequency domain so that $\mathcal{H}^t_\omega[\phi_i(x)]$ describes the distributed moment per unit length due to fluid-structure interactions when the beam is vibrating along mode $\phi_i(x)$ at a frequency ω.

In compact form, this expression can be rewritten as

$$[\boldsymbol{K} - \omega^2 \boldsymbol{M} - \boldsymbol{H}^t(\omega)]\hat{\boldsymbol{q}} = \hat{\boldsymbol{m}} \tag{3}$$

where $\boldsymbol{K}$ and $\boldsymbol{M}$ are the traditional stiffness and mass matrices of the system, $\hat{\boldsymbol{q}}$ is the vector of modal coefficients, $\hat{\boldsymbol{m}}$ is the modal forcing vector. The main contribution of this work is the complex-valued modal hydrodynamic function matrix $\boldsymbol{H}^t(\omega)$, whose entries are

$$[\boldsymbol{H}^t(\omega)]_{ji} = h_{ji}(\omega) = \int_0^L \mathcal{H}^t_\omega[\phi_i(x)]\phi_j(x)\mathrm{d}x \tag{4}$$

This term is novel, and physically describes the projection of the hydrodynamic moment due to vibration along mode i onto mode j. Energy considerations reported elsewhere (and numerical experimentation) also demonstrate that the matrix $\boldsymbol{H}^t(\omega)$ is symmetric but not Hermitian, so that $h_{ji} = h_{ij}$. As opposed to local formalisms common in the literature, the global motion of the structure is used for the calculation of the hydrodynamic loading at any point and therefore our approach naturally takes into account boundary conditions, edge effects, and finite aspect ratios in the fluid-structure interaction problem.

As shown later, $\boldsymbol{H}^t(\omega)$ is a complex-valued matrix that displays a complicated dependence on the frequency ω. From Eq. (3), it can be deduced that the real part of $\boldsymbol{H}^t(\omega)$ captures the effect of an hydrodynamic added mass moment of inertia that will shift the "wet" resonance frequencies of the system. Similarly, the imaginary part of $\boldsymbol{H}^t(\omega)$ describes the hydrodynamic damping and captures the reduction of the vibration amplitude at wet resonance, as compared to in-vacuo vibrations. Both these effects will be discussed in detail in Section 3. In the next subsection, we will detail the calculation of the terms h_{ij} from the solution of the fluid problem.

2.2 Oscillatory Stokeslet solution of the fluid problem

The calculation of the hydrodynamic load due to a prescribed structural deformation $w(x,y,t)$ at a frequency ω proceeds by following in part the approach in [16]. Briefly, the hydrodynamic regime of interest is the unsteady Stokes flow, for which convective nonlinearities are neglected. The fluid is incompressible, with density ρ_f and viscosity μ_f, and gravity or body forces are neglected. The structure is subject to harmonic and vanishingly small-amplitude steady state torsional vibrations. The ensuing structural velocity, through the no-slip condition, is used as boundary conditions for the fluid velocity field. Under these assumptions, the evolution of the fluid velocity field is also time-harmonic. Building on the oscillatory Stokeslets formalism in [13, 14], the governing equations are

$$\mathrm{i}\omega\hat{w}(\bar{\boldsymbol{x}}) = \frac{1}{8\pi}\int_D \hat{P}(\boldsymbol{x},\omega)S_{33}(\boldsymbol{x},\bar{\boldsymbol{x}};\alpha)\,\mathrm{d}\boldsymbol{x} \tag{5}$$

where D is the domain of the beam $D = (0,L)\times(-b/2,b/2)$. Eq. (5) relates the phasor of the solid velocity $\mathrm{i}\omega\hat{w}(\bar{\boldsymbol{x}})$ at a point $\bar{\boldsymbol{x}} = (\bar{x},\bar{y})$ on the structure to the phasor of the net hydrodynamic load, or net traction, $\hat{P}(\boldsymbol{x},\omega)$ at a different point $\boldsymbol{x} = (x,y)$ on the beam, via a kernel $S_{33}(\boldsymbol{x},\bar{\boldsymbol{x}},\alpha)$ which is only a function of the distance $r = |\boldsymbol{x}-\bar{\boldsymbol{x}}|$ and of the nondimensional parameter $\alpha = \sqrt{\omega\rho_f b^2/\mu_f}$. In [16], $S_{33}(\boldsymbol{x},\bar{\boldsymbol{x}},\alpha)$ was rewritten as $S_{33}(\boldsymbol{x},\bar{\boldsymbol{x}},\alpha) = A(|\boldsymbol{x}-\bar{\boldsymbol{x}}|,\alpha)$, with

$$A(r,\alpha) = 2\frac{e^{-\sqrt{\mathrm{i}}\alpha r}}{r}\left(1+\frac{1}{\sqrt{\mathrm{i}}\alpha r}-\frac{\mathrm{i}}{\alpha^2 r^2}\right)+\frac{2\mathrm{i}}{\alpha^2 r^3} \tag{6}$$

For a given velocity profile, aspect ratio, and a prescribed ω (or, equivalently, α) Eq. (5) can be solved to determine the net hydrodynamic traction by using the boundary element technique in [16]. Here, we solve Eq. (5) when the structure velocity is produced by vibration along a designated mode, that is,

$$\mathrm{i}\omega\bar{y}\phi_i(\bar{x}) = \frac{1}{8\pi}\int_{\boldsymbol{D}} \hat{P}_{\phi_i}(\boldsymbol{x},\omega)S_{33}(\boldsymbol{x},\boldsymbol{x'};\alpha)\,\mathrm{d}\boldsymbol{x} \tag{7}$$

where we have used $\hat{P}_{\phi_i}$ to indicate the net traction due to vibration along mode ϕ_i. An example of such calculation is shown in Fig. 2 which displays the real and imaginary part of the phasor of $\hat{P}_{\phi_1}$ at a representative frequency. Note here, the complicated (and in fact singular) behavior of the traction in the vicinity of the boundaries. These effects, that are known to exist, cannot be captured by traditional local approaches such as those in [10] based on two-dimensional approximations of the fluid problem, see [5, 6].

Once the net traction has been numerically determined, the hydrodynamic moment per unit length is $\mathcal{H}^t_\omega[\phi_i] = \int_{-b/2}^{b/2} y\hat{P}_{\phi_i}\mathrm{d}y$, so that its projection on the beam modes is

$$h_{ij}(\omega) = \int_0^L \int_{-b/2}^{b/2} y\hat{P}_{\phi_i}(x,y,\omega)\mathrm{d}y\,\phi_j(x)\mathrm{d}x \tag{8}$$

Importantly, notice that because of the complicated two-dimensional distribution of the traction, the moment is not proportional to a mode shape, as is postulated in the local approaches. This results in non-zero off-diagonal components for the modal hydrodynamic function matrix, which have never been identified before for torsional vibrations. This finding is an important difference between our present theory and local approaches.

It is convenient to normalize the h_{ij} terms by introducing $\tilde{h}_{ij} = h_{ij}/(\pi\rho_f\omega^2 b^4 L/8)$. In this way, $\tilde{h}_{ij}$ depend only on a nondimensional frequency parameter $\beta = \alpha^2/(2\pi)$ and the aspect ratio $\Lambda = L/b$. As in the fluid problem the structural properties are not specified, ω should be regarded as a free parameter. Thus, the components of the modal hydrodynamic function matrices can be determined in this way for a variety of frequencies and aspect ratios of interest. We use interpolation between calculated values to estimate $\boldsymbol{H}^t(\omega)$ in

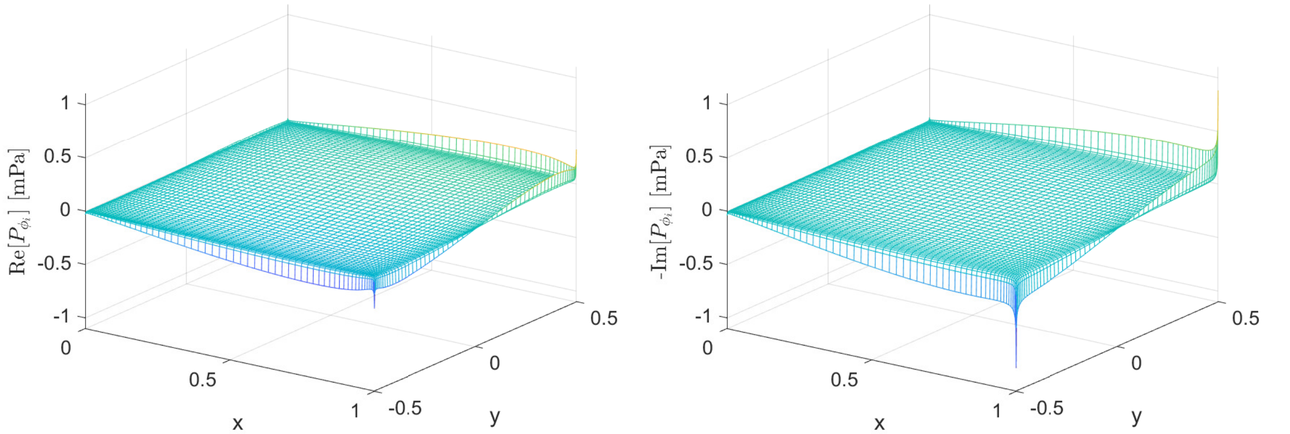

Fig. 2. Real and negative imaginary part of the net traction phasor profile on the surface of the beam for vibration along the first mode ϕ_1 at $\alpha = \sqrt{2\pi \cdot 100}$, for aspect ratio $\Lambda = 1$.

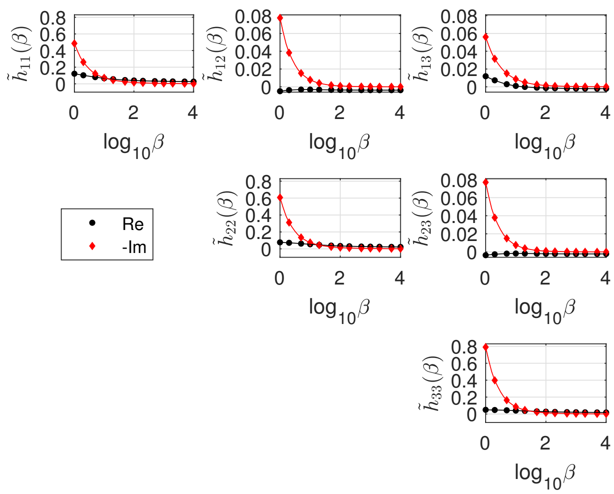

Fig. 3. Representative components of the modal hydrodynamic function matrix $\tilde{\boldsymbol{H}}$ for aspect ratio $\Lambda = 1$. Note the non-zero off-diagonal components.

the solution of Eq. (3) for frequencies that have not been explicitly calculated. An example of the calculation of the $\tilde{h}_{ij}$ for $\Lambda = 1$ over a broad range of β values is displayed in Fig. 3, which also clearly displays the non-diagonal nature of the operator $\mathcal{H}^t_\omega$ even when its components are specified with respect to an orthogonal basis. While conventional methods only consider diagonal terms, off-diagonal terms cannot be ignored, as they can be 10-15% of the diagonal values at low frequencies.

3 RESULTS

3.1 Experimental validation

To provide experimental validation for our new nonlocal theory, in Fig. 4 we show a comparison between the predictions of the present model against experimental measurements of torsional vibrations in [11], for the first torsional mode of a flexible submerged cantilever. Note that in [11], spurious effects of the cantilever deflection were eliminated from the torsion data via postprocessing of the experimental measurements. The material used in the experiments is a 5-mil thick (127 μm) Mylar sheet. Dimensions are $L = 150$ mm and $b = 25$ mm ($\Lambda = 6$). Material properties, obtained from the manufacturer, are $E = 5$ GPa, $\nu = 0.38$, and $\rho = 1390\,\text{kg/m}^3$. Structural damping, as determined in [11] from in-air free vibrations, is set to $\eta = 0.012$. Thus, a complex shear modulus $G = E(1+i\eta)/[2(1+\nu)]$ is used in the construction of the stiffness matrix in Eq. (2). Fluid properties are those for standard water at room temperature. Experimental data are obtained from the top-right panel of Fig. 9 of [11] which correspond to small amplitude of oscillation for which the response of the system is presumed to be linear.

To study the base excitation response of the torsional system, the moment per unit length m_t term in Eq. (2) is specialized to $m_t = (\omega^2 \rho_s I_t + \mathcal{H}^t_\omega[\mathbf{1}])\hat{B}(\omega)$, where $\hat{B}(\omega)$ is the phasor of the base excitation (possibly, a frequency-dependent real number describing the amplitude of the base angle of rotation) and $\mathcal{H}^t_\omega[\mathbf{1}]$ is the hydrodynamic loading due to rigid body rotation of the plate at the excitation frequency ω. Note that this term is also a novel corollary of the present theory and is calculated from Eq. (7) by substituting $\phi(x)$ with the function identically equal to 1 along the axis of the beam. Correct estimation of this term, which is also nonlocal, is important for the accurate evaluation of the magnitude of the base excitation and, therefore, of the response of the elastic system. Remarkably, this term cannot be predicted with the local formulation as in [10, 11].

Predictions of the present nonlocal theory are expressed as the frequency response function of the tip twist angle normalized by the amplitude of the base excitation, that is $\left|\sum_i \hat{q}_i(\omega)\phi_i(L)/\hat{B}(\omega)\right|$, in Fig. 4, over the frequency range $[1,6]$ Hz. Despite the experimental scatter past the resonance peak, which is likely due to experimental uncertainties in the data in [11], the present theory is in excellent agreement with

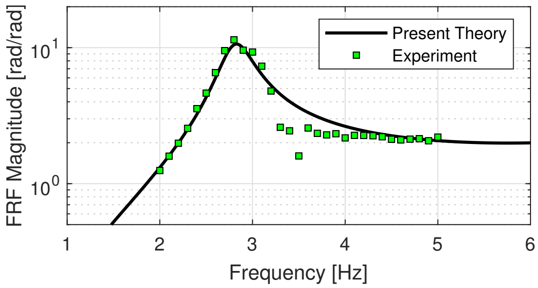

Fig. 4. Comparison of the predictions of the nonlocal theory against the experimental measurement reported in [11] for the first torsional mode.

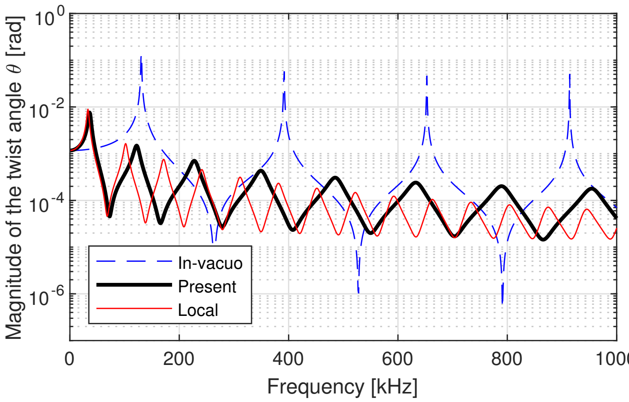

Fig. 5. Frequency response functions of the submerged cantilever beam for aspect ratio $\Lambda = 1$. The thin dashed line indicates the in-vacuo FRF of the structure.

the data from the literature, in terms of both the qualitative shape of the FRF curve, as well as the quantitative predictions of the natural frequency, quality factor, and amplitude of the excitation and response. Importantly, no tuning parameters are used in the derivation of these results. This finding further confirms and validates our approach.

3.2 Numerical results and exploration of the theory

The characteristics of the present theory are discussed with reference to underwater torsional vibrations of a silicon microcantilever beam ($E = 169\,\text{MPa}$, $\nu = 0.33$, $\rho = 2320\,\text{kg/m}^3$) with dimensions $L = 200\,\mu\text{m}$, $h = 2\,\mu\text{m}$, and $b = 200\,\mu\text{m}$. Fluid properties are $\rho_f = 997\,\text{kg/m}^3$ and $\mu_f = 8.59 \times 10^{-4}\,\text{Pa} \cdot \text{s}$. The first twenty modes are used in all calculations. The first four undamped in-vacuo torsional modes of the cantilever appear in the frequency range $[0, 1000]$ kHz, at approximately 131 kHz, 392 kHz, 653 kHz, and 914 kHz, along with the first eight estimated "wet" modes as shown in Fig. 5. The fifth in-vacuo mode occurs at approximately 1175 Hz.

Fig. 5 displays the magnitude of the twist angle FRF produced by a time-varying harmonic moment of magnitude $b \cdot 1\,\mu\text{N} \cdot \text{m}$ applied at the free tip of the cantilever. We display the magnitude of this FRF for in-vacuo vibrations and for submerged vibrations as predicted by the local theory

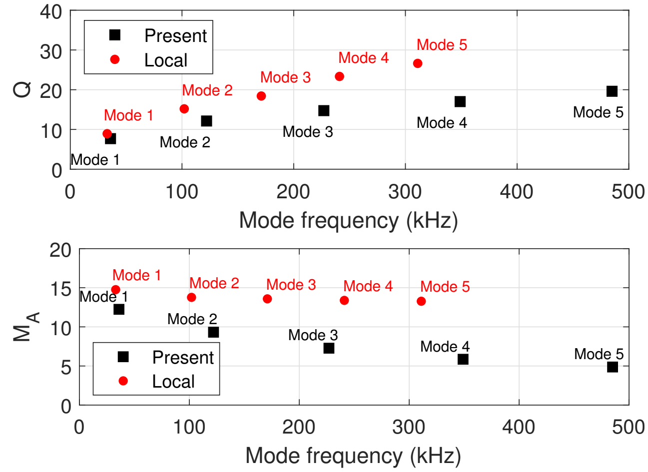

Fig. 6. Quality factor Q and added mass M_A for aspect ratio $\Lambda = 1$.

in [10] and our nonlocal theory, for aspect ratio $\Lambda = 1$. For the first "wet" mode, the local and nonlocal theories predict the damped frequencies at 33 kHz and 36 kHz, with a difference of 8%. For "wet" mode 2, the local theory predicts a damped resonance at 102 kHz, while the present theory suggests 122 kHz. The local theory underestimates the natural frequency by more than 25%. As the mode number increases more, the discrepancy further increases, up to 36% for the fifth "wet" mode.

Further quantitative insight for our proposed solution can be obtained by evaluating the quality factors and the added mass of the first five "wet" modes for $\Lambda = 1$, see Fig. 6. These parameters are estimated as $Q = \omega_p/(\omega_2 - \omega_1)$; and $M_A = (\omega_v/\omega_w)^2 - 1$. Here, quality factors are estimated with the half-power point method [15] where ω_p denotes the frequency of the peak response, ω_1 and ω_2 are the frequencies of the lower and upper half-power points. For the added mass, the subscripts v or w indicate in-vacuo or "wet", respectively, for the resonance frequencies. For the first "wet" mode, the local and nonlocal theory predict the quality factors $Q = 8.93$ at 33 kHz with $M_A = 14.76$ and $Q = 7.69$ at 36 kHz with $M_A = 12.24$, respectively. The local theory overestimates the damping and the added mass by 16% and 21%. For wet mode 2, the local theory predicts the damping as $Q = 15.19$ at 102 kHz with $M_A = 13.77$, while the present theory with "wet" hydrodynamic operator obtains $Q = 12.12$ at 122 kHz with $M_A = 9.32$. The local theory overestimates the quality factor and the added mass predicted by the nonlocal theory by more than 25% and 50%. As mode number increases, the discrepancy increases, up to 36% in damping and 170% in the added mass at the fifth "wet" mode.

An important feature of our method is that the vibration shape is not imposed a priori to calculate the hydrodynamic load, as in [7, 16], but the actual shape is instead recovered from the solution of Eq. (3). As such, the shapes at resonance are not the in-vacuo mode shapes and they differ substantially from the predictions of the local theory, as shown in Fig. 7. The main source of discrepancy is in the non-diagonal nature of the $\boldsymbol{H}^t(\omega)$ matrix, and in the way all

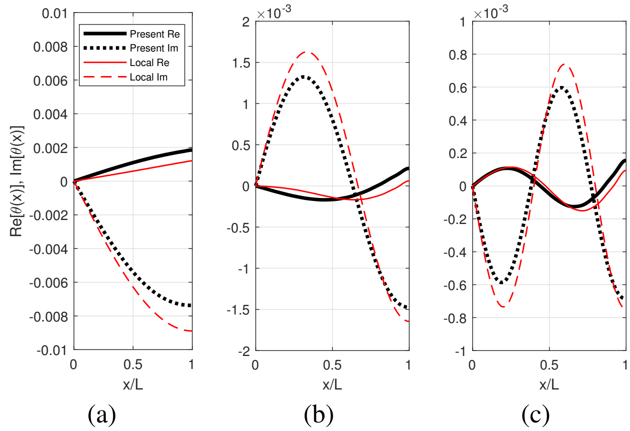

Fig. 7. Deformed shapes at "wet" resonance for $\Lambda = 1$. In (a): mode 1; in (b): mode 2; in (c): mode 3. Note the shift of the nodal locations.

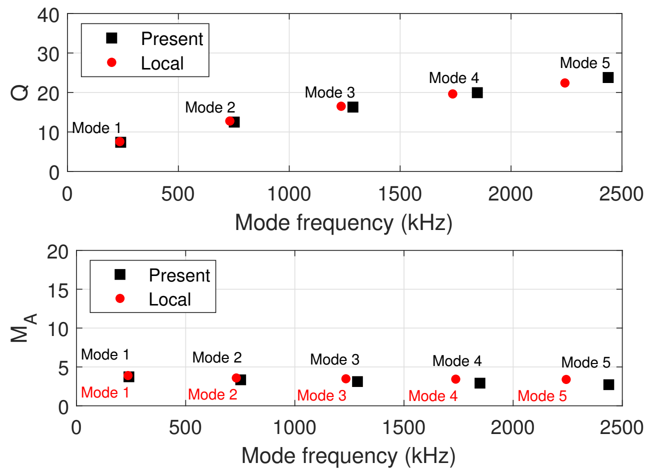

Fig. 8. Quality factor Q and added mass M_A for aspect ratio $\Lambda = 4$.

modes are coupled and excited by the nonlocal fluid loading. This phenomenon cannot be predicted by the local theory.

Analysis of the cantilever responses clearly shows that the current approach differs significantly from the local theory, especially for high mode numbers. This conclusion is in line with the findings in [6] and originates from neglecting the entire structure's movement in the estimation of the hydrodynamic loading at each location along the cantilever axis. While the local approach is generally accurate for slender structures and low modes, it fails to produce accurate results for the cases of interest in this study. However, we here investigate its limits of validity by considering a second cantilever with $b = 50\mu$m so that the aspect ratio is a less extreme $\Lambda = 4$. Predictions on added masses and quality factors are displayed in Fig. 8. These demonstrate that the nonlocal theory is close to the local theory for damping especially for the first two "wet" modes. These are with $Q = 7.38$ at 240 kHz and $Q = 12.50$ at 752 kHz, whereas the local theory predicts $Q = 7.55$ at 236 kHz and $Q = 12.76$ at 732 kHz. These values correspond to 2.3% and 4.3% differences for the damping, respectively. For the added masses, the estimation of the local and nonlocal theories are 3.89 and 3.58 vs. 3.73 and 3.34 for the first and second "wet" modes, respectively. These values correspond to 4.3% and 7.2% differences for the first two "wet" modes, respectively. For higher modes, the difference in damping increases up to 5.8% at the fifth "wet" mode where the difference is risen to 25% for the added mass. Interestingly, for the fourth and fifth mode, the local theory seems to underestimate the quality factors instead of overestimating as in the first three modes.

4 CONCLUSION

In this paper, we developed a nonlocal theory for the small amplitude torsional vibrations of a submerged cantilever beam. The predictions of our theory show excellent agreement with experiments. Comparison with the classical local theory of [10] highlights important deviations for low aspect ratios and high mode number. This result is theoretically expected as the local theory cannot predict boundary effects due to finite aspect ratio.

In turn, our theory is "exact", as the fluid treatment is fully three-dimensional and correctly captures the full loading on the entire structure. Approximations in our theory are related to numerical truncation and can be systematically removed. While accurate, our theory is numerically inexpensive, as the FSI problem is solved once and for all, for prototypical vibration scenarios, and its results are seamlessly integrated in conventional structural models via the novel concept of nonlocal modal hydrodynamic function matrix.

We believe that our nonlocal theory provides a novel perspective on hydrodynamic loading in high-frequency torsional vibrations of small aspect ratio structures, of particular interest for MEMS applications in liquid. We remark that this work focuses on the beam torsional behavior with the ad-hoc "mechanics of materials" theory that is extensively used in practice, following the fundamental contributions of [10]. Nonlocal hydrodynamics integrated in plate-like mechanics, which may be dominant for lower aspect ratio structures, will be presented elsewhere.

ACKNOWLEDGMENTS

This material is based upon work supported by the National Science Foundation under Grant CMMI-1847513.

References

[1] Maali, A., Hurth, C., Boisgard, R., Jai, C., Cohen-Bouhacina, T., and Aimé, J.-P., 2005. "Hydrodynamics of oscillating atomic force microscopy cantilevers in viscous fluids". *Journal of Applied Physics,* **97**(7), p. 074907.

[2] Manzaneque, T., Ruiz-Díez, V., Hernando-García, J., Wistrela, E., Kucera, M., Schmid, U., and Sánchez-Rojas, J. L., 2014. "Piezoelectric MEMS resonator-based oscillator for density and viscosity sensing". *Sensors and Actuators A: Physical,* **220**, pp. 305–315.

[3] Eastman, A., and Kimber, M. L., 2014. "Flow shaping and thrust enhancement of sidewall bounded oscillating cantilevers". *International Journal of Heat and Fluid Flow,* **48**, pp. 35 – 42.
[4] Behbahani, S. B., and Tan, X., 2016. "Bio-inspired flexible joints with passive feathering for robotic fish pectoral fins". *Bioinspiration & biomimetics,* **11**(3), p. 036009.
[5] Tuck, E. O., 1969. "Calculation of unsteady flows due to small motions of cylinders in a viscous fluid". *Journal of Engineering Mathematics,* **3**, pp. 29–44.
[6] Sader, J. E., 1998. "Frequency response of cantilever beams immersed in viscous fluids with applications to the atomic force microscope". *Journal of applied physics,* **84**(1), pp. 64–76.
[7] Gesing, A., Platz, D., and Schmid, U., 2022. "A numerical method to determine the displacement spectrum of micro-plates in viscous fluids". *Computers and Structures,* **260**, p. 106716.
[8] Atkinson, C., and de Lara, M. M., 2007. "The frequency response of a rectangular cantilever plate vibrating in a viscous fluid". *Journal of Sound and Vibration,* **300**(1-2), feb, pp. 352–367.
[9] Shen, N., Chakraborty, D., and Sader, J. E., 2023. "Frequency response of cantilevered plates of small aspect ratio immersed in viscous fluids". *Journal of Applied Physics,* **133**(3), jan, p. 034501.
[10] Green, C. P., and Sader, J. E., 2002. "Torsional frequency response of cantilever beams immersed in viscous fluids with applications to the atomic force microscope". *Journal of Applied Physics,* **92**(10), pp. 6262–6274.
[11] Aureli, M., Pagano, C., and Porfiri, M., 2012. "Nonlinear finite amplitude torsional vibrations of cantilevers in viscous fluids". *Journal of Applied Physics,* **111**(12), p. 124915.
[12] Gesing, A., Platz, D., and Schmid, U., 2022. "Viscous fluid-structure interaction of micro-resonators in the beam-plate transition". *Journal of Applied Physics,* **131**, p. 134502.
[13] Clarke, R., Jensen, O., and Billingham, J., 2008. "Three-dimensional elastohydrodynamics of a thin plate oscillating above a wall". *Physical Review E,* **78**(5), p. 056310.
[14] Pozrikidis, C., 1989. "A singularity method for unsteady linearized flow". *Physics of Fluids A: Fluid Dynamics,* **1**(9), pp. 1508–1520.
[15] Meirovitch, L., 1967. *Analytical Methods in Vibrations*. MacMillan, London.
[16] Ahsan, S. N., and Aureli, M., 2018. "Three-dimensional analysis of hydrodynamic forces and power dissipation in shape-morphing cantilevers oscillating in viscous fluids". *International Journal of Mechanical Sciences,* **149**, pp. 436–451.